the beads for 90 min at 4°C, washed four times with buffer B (buffer A plus 100 mM NaCl), resuspended in loading buffer, and fractionated by SDS–8% polyacrylamide gel electrophoresis (PAGE). For GST fusion protein interaction assays, cDNAs encoding full-length or truncated BARD1 were inserted into pGEX-2TK and expressed in *E. coli*. Proteins were purified by binding to and eluting from glutathione-agarose beads, and 1 mg of the indicated protein was incubated with ^{35}S-labeled CstF-50. Conditions were as in the coimmunoprecipitation assays, except washing was with buffer B containing 300 mM NaCl.

24. HeLa cell NE was subjected to a 20% to 40% $(NH_4)_2SO_4$ cut and fractionated by Superose-6 chromatography (*25*). Selected fractions were analyzed by immunoblotting with mAbs targeted against BARD1 (EE 6) (*16*), CstF-64 (*9*), or BRCA1 (MS110) (*33*). NE and fractions eluting from Superose-6 were immunoprecipitated with the anti-BARD1 polyclonal antibody, or the anti-CstF64 or BRCA1 mAbs, bound to protein A–Sepharose beads. Immunoprecipitations were carried out in buffer B at 4°C for 90 min, and washing was with buffer B. Aliquots of pellets and supernatants were analyzed by SDS-PAGE and immunoblotting. The anti-BARD1 and CstF-64 antibodies did not cross-react with CstF-64 and BARD1, respectively, as judged by experiments with purified (BARD1-free) CstF and recombinant GST–BARD1 (*22*).
25. Y. Takagaki, L. C. Ryner, J. L. Manley, *Cell* **52**, 731 (1988).
26. ^{32}P-labeled pre-mRNA substrates were prepared as in (*34*). Cleavage assays in NE were carried out in reaction mixtures containing 0.2 to 0.5 ng of labeled RNA, 250 ng of tRNA, 0.25 unit of RNasin (Promega), 9.6 mM Hepes·NaOH (pH 7.9), 9.6% glycerol, 24 mM $(NH_4)_2SO_4$, 20 mM creatine phosphate, 0.24 mM dithiothreitol, 2.5% polyvinyl alcohol, 0.24 mM phenylmethylsulfonyl fluoride, and either 2 mM EDTA or 1 mM $MgCl_2$. NE and added proteins or antibodies were preincubated for 15 min at 30°C, after which the pre-mRNA was added and incubation continued for an additional 90 min. RNA products were isolated and fractionated on 5% polyacrylamide, 8.3 M urea gels.
27. R. Scully *et al.*, *Proc. Natl. Acad. Sci. U.S.A.* **94**, 5605 (1997).
28. R. Scully *et al.*, *Cell* **88**, 265 (1997).
29. A. Shinohara, H. Ogawa, T. Ogawa, *Cell* **69**, 457 (1992); P. Baumann, F. E. Benson, S. C. West, *ibid.* **87**, 757 (1996).
30. E. Maldonado *et al.*, *Nature* **381**, 86 (1996).
31. L. C. Gowen *et al.*, *Science* **281**, 1009 (1998).
32. E. Warbrick, W. Heatherington, D. P. Lane, D. M. Glover, *Nucleic Acids Res.* **26**, 3925 (1998).
33. R. Scully *et al.*, *Science* **272**, 123 (1996).
34. Y. Hirose and J. L. Manley, *J. Biol. Chem.* **272**, 29636 (1997).
35. J. Chen, D. Livingston, R. Baer, personal communication.
36. Supported by National Institutes of Health (NIH) grant GM28983 to J.L.M. and an NIH Fogarty Fellowship to F.E.K. We thank Y. Takagaki for CstF plasmids and antibodies; R. Baer for BARD1 and BRCA1 encoding plasmids and anti-BARD1 antibodies; J. Chen and D. Livingston for the anti-BRCA1 antibody; R. Brent for yeast two-hybrid reagents; Y. Hirose for HeLa nuclear extract; and C. Prives, R. Baer, Y. Hirose, and R. Tacke for advice and discussions.

25 June 1999; accepted 29 July 1999

Control of Circadian Rhythms and Photoperiodic Flowering by the *Arabidopsis GIGANTEA* Gene

Deok Hoon Park,[1]* David E. Somers,[2]* Yang Suk Kim,[1] Yoon Hi Choy,[1] Hee Kyun Lim,[1] Moon Soo Soh,[1] Hyo Jung Kim,[1] Steve A. Kay,[2] Hong Gil Nam[1]†

Photoperiodic responses in plants include flowering that is day-length–dependent. Mutations in the *Arabidopsis thaliana GIGANTEA* (*GI*) gene cause photoperiod-insensitive flowering and alteration of circadian rhythms. The *GI* gene encodes a protein containing six putative transmembrane domains. Circadian expression patterns of the *GI* gene and the clock-associated genes, *LHY* and *CCA1*, are altered in *gi* mutants, showing that GI is required for maintaining circadian amplitude and appropriate period length of these genes. The *gi-1* mutation also affects light signaling to the clock, which suggests that GI participates in a feedback loop of the plant circadian system.

The circadian clock system is a self-sustained biological oscillator with a period of ~24 hours that operates ubiquitously in animals, plants, and microorganisms (*1, 2*) and controls a wide range of rhythmic processes (*3, 4*). In plants, the circadian clock controls daily changes of photosynthetic activities, leaflet movement, cell growth, and expression of several genes, including the chlorophyll a/b binding protein (*CAB*) genes (*2, 5*). Several components regulating the circadian system have been genetically defined in *Arabidopsis thaliana* (*6, 7*). However, molecular components controlling the plant circadian system are largely unknown, except for the two clock-associated factors, LHY and CCA1 (*8, 9*).

The ability to perceive changes in day length (*7, 10–12*), photoperiodism, is essential for organisms to recognize seasonal changes and is associated with the circadian clock system (*4, 7–9*). *Arabidopsis* is a facultative long-day plant, flowering in a fewer number of days under long photoperiods than under short photoperiods. Certain alleles of the *Arabidopsis gi* mutants are insensitive to photoperiod (*11, 13, 14*). Here, we report an important role for GI in plant circadian function and molecular nature of the *Arabidopsis gi* mutations.

Cotyledons and leaves of *Arabidopsis* show circadian movement, rising and falling in relative position during subjective night and day, respectively (*7*). Measurement of leaf movement rhythms (*15*) revealed that both the *gi-1* and *gi-2* mutants have shorter circadian periods than wild-type plants (Fig. 1, A and B, and Table 1).

Expression of the *CAB2* gene is under the control of the circadian clock in *Arabidopsis*. To characterize the effects of the *gi* mutations on the circadian system, we crossed the clock-controlled reporter construct, *cab2::luciferase* (*cab2::luc*) (*6*), into the *gi-1* and *gi-2* backgrounds. Both mutants alter the circadian period of *cab2::luc* expression (Fig. 1C and Table 1) (*15*). The period is substantially shorter in the homozygous *gi-1* mutant than in the wild type, and this effect is dependent on gene dosage (Fig. 2A and Table 1). In contrast, the *gi-2* mutation causes the period to lengthen and is fully recessive (Fig. 2B and Table 1). Luminescence cycling in the *gi-2* background remained in phase with the wild type for up to 60 hours after transfer to continuous white light (LL), after which the period lengthened (Fig. 1C) (*15, 16*). There was no apparent lag in the period-shortening effects of the *gi-1* mutation (Fig. 1C). Both mutations caused an abnormally rapid damping of rhythm amplitude.

We cloned the *GI* gene with a map-based approach. The *GI* locus is linked to the *THIAMINE REQUIRING 1* (*TH1*) locus on chromosome 1 (*17*). We thus used the *TH1* gene to screen an *A. thaliana* bacterial artificial chromosome (BAC) library, identifying the BAC clone T23L3 (*18*). Subsequent probing with T23L3 identified two contiguous BAC clones, T14K14 and T22J18 (*19*). The *gi-1* and *gi-2* alleles were generated by x-ray mutagenesis (*13*), which frequently generates deletion mutants. When wild-type (Columbia), *gi-1*, and *gi-2* genomic DNA were digested with Stu I and probed with theT22J18 clone, two restriction fragments (7.1 and 1.1 kb, respectively) detected in the wild-type and *gi-2* lines appeared as a single 8.2-kb band in the *gi-1* mutant (*19*). End sequences of the 7.1- and 1.1-kb fragments (*20*) matched a genomic sequence (GenBank accession number Y12227) that contains a predicted open reading frame (ORF) of 1167 amino acids. Sequence comparisons in this region between the wild-type, *gi-1*, and *gi-2* lines revealed small deletions within the predicted ORF in both mutants (*19*).

[1]Department of Life Science, Pohang University of Science and Technology, Pohang, Kyungbuk, 790-784, Korea. [2]Department of Cell Biology and National Science Foundation Center for Biological Timing, The Scripps Research Institute, 10550 North Torrey Pines Road, La Jolla, CA 92307, USA.

*These authors contributed equally to this work.
†To whom correspondence should be addressed. E-mail: hgn@bric.postech.ac.kr

Using a probe generated by polymerase chain reaction (PCR), we identified a full-length cDNA clone of 3522 base pairs (bp) (GenBank accession number AF105064) that codes for a 1173–amino acid polypeptide (*19, 21, 22*). The *gi-1* mutant has a 5-bp deletion, resulting in a putative premature translation stop with a loss of the 171 COOH-terminal amino acids (*19*). The *gi-2* mutant has a 7-bp deletion, resulting in a putative premature translation stop with a loss of all but the 142 NH_2-terminal amino acids of the polypeptide and an addition of 16 new amino acids at the COOH-terminus.

The flowering time phenotype suggests that *gi-1* is a weak allele, still possessing some photoperiodic responses, whereas the *gi-2* mutation acts as a strong allele, showing complete insensitivity to photoperiod (*11, 14*). The sequence data are consistent with these phenotypes. A loss of most of the coding region in the *gi-2* mutant is likely to produce a nonfunctional polypeptide. In contrast, the *gi-1* mutant lacks only a small portion of the COOH-terminus of GI, and a peptide with partial function or a modified activity may still be produced. *GI* appears to be a single-copy gene and is expressed in all the organs examined (*19*). The predicted normal polypeptide contains six potential membrane-spanning domains, strongly suggesting that GI is a membrane protein (*19*). A database search with the predicted peptide sequence did not reveal any related sequences.

We tested the effects of the *gi* mutations on *GI* expression and on two clock-associated genes, *CCA1* and *LHY* (*8, 9*). After entrainment under 12 hours of light and 12 hours of

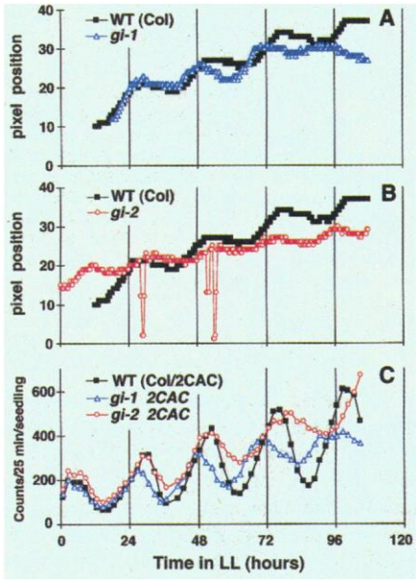

Fig. 1. Representative traces of (**A** and **B**) circadian rhythms of leaf movement and (**C**) *cab2::luc* expression in wild-type (WT), *gi-1*, and *gi-2* mutant backgrounds under constant white light (LL). Plants were germinated and grown for 6 to 7 days under light and dark cycles as previously described (*25*) before they were transferred to continuous white light for >110 hours. Leaf movements were recorded (*7*), and luminescence assays were conducted (*25*) to obtain period estimates as previously described (*6, 27*). Individual bioluminescent F_3 lines homozygous for the *gi-1* (*gi-1 2CAC*) or *gi-2* (*gi-2 2CAC*) mutations were isolated from crosses to a *cab2::luc*-expressing line (2CAC, C24 ecotype) (*6, 28*). WT (Col), Columbia ecotype; WT (Col/2CAC), *cab::luc* introgressed five times into the Columbia ecotype.

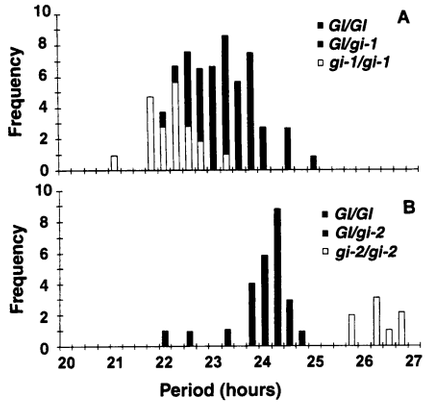

Fig. 2. Period length distribution in F_2 populations segregating for (**A**) *gi-1* or (**B**) *gi-2* (*28*). Plants were entrained and assayed as described in Fig. 1. Period bins are labeled with the upper bound.

Table 1. Circadian periods of leaf movement and *cab2::luc* expression in the *gi* mutants. Period length estimates (variance-weighted mean period ± variance-weighted SD) were obtained as described (*6, 27*). *n*, number of rhythmic leaves (leaf movement) or seedlings (*cab2::luc*) contributing to a mean; Col, Columbia ecotype; *gi-1* F_2 and *gi-2* F_2 indicate the segregating population from which the indicated genotypic subclass was sampled (*28*); ND, not determined.

Genotype	Mean period length (hours)	
	Leaf movement (*n*)	*cab2::luc* (*n*)
Wild type	(Col) 25.2 ± 0.2 (18)	(*gi-1* F_2) 23.4 ± 0.4 (21)
gi-1/gi-1	(Col) 22.4 ± 0.3 (4)	(*gi-1* F_2) 21.8 ± 0.4 (21)
GI/gi-1	ND	(*gi-1* F_2) 22.9 ± 0.6 (27)
Wild type	(Col) 25.2 ± 0.2 (18)	(*gi-2* F_2) 24.0 ± 0.6 (8)
gi-2/gi-2	(Col) 21.1 ± 0.7 (7)	(*gi-2* F_2) 26.2 ± 0.5 (10)
GI/gi-2	ND	(*gi-2* F_2) 23.9 ± 0.4 (18)

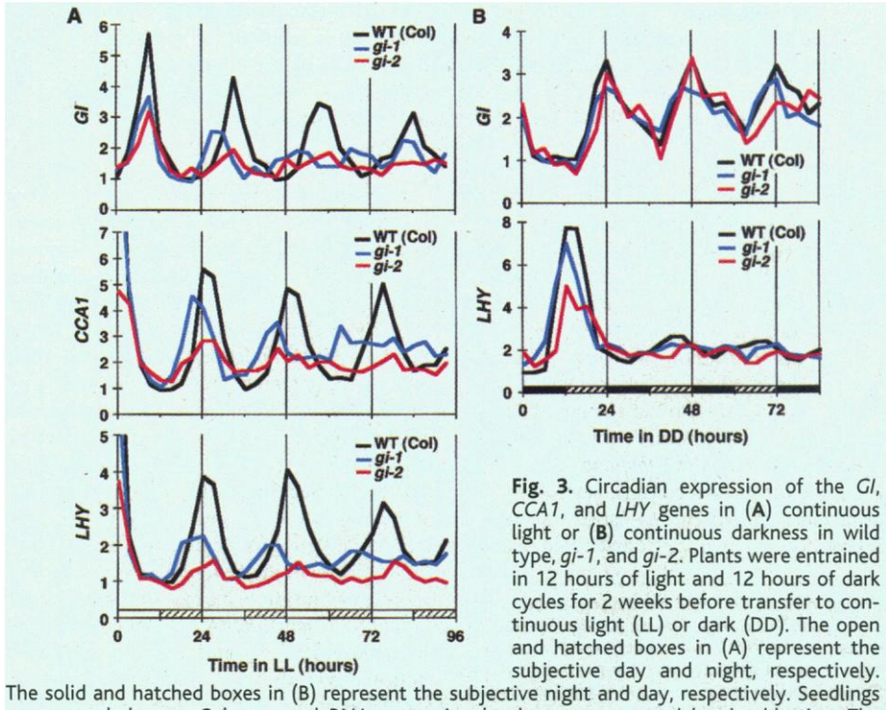

Fig. 3. Circadian expression of the *GI*, *CCA1*, and *LHY* genes in (**A**) continuous light or (**B**) continuous darkness in wild type, *gi-1*, and *gi-2*. Plants were entrained in 12 hours of light and 12 hours of dark cycles for 2 weeks before transfer to continuous light (LL) or dark (DD). The open and hatched boxes in (A) represent the subjective day and night, respectively. The solid and hatched boxes in (B) represent the subjective night and day, respectively. Seedlings were sampled every 3 hours, and RNA expression levels were measured by dot blotting. The *Brassica BGB1* clone (*29*) corresponding to the *Arabidopsis AtarcA* gene was used as a control. Values are normalized to the lowest value of the wild-type samples in each set. The LL and DD experiments were performed three times and twice, respectively. Representative data are shown.

darkness (LD), a strong free-running oscillation of *GI* gene expression persisted in LL in the wild type (Fig. 3A), with peak expression in the subjective evening and with a mean estimated period length of 24.9 ± 0.5 hours (*23*). In contrast, the *gi-1* mutation confers a shorter period (21.3 ± 1.4 hours) than the wild type, whereas in *gi-2* the abundance of *GI* transcript cycles at low amplitude with a longer period length (26.3 ± 3.2 hours) (*23*). Unlike other clock component genes that negatively regulate their own expression (*3, 24*), the expression level of the *GI* gene is much lower in both *gi* alleles than in the wild type, suggesting that GI positively regulates its own expression.

The *Arabidopsis CCA1* and *LHY* genes encoding the MYB-related transcription factors that may be central to normal circadian function (*8, 9*) show circadian expression patterns. The circadian expression patterns of both genes were altered in the *gi* mutants (Fig. 3A). Consistent with the *cab2::luc* results (Table 1 and Fig. 1C), the *gi-1* mutation shortened the free-running period (*23*) of both cycling transcripts (22.7 ± 1.2 and 21.8 ± 0.9 hours for *CCA1* and *LHY*, respectively), relative to wild type (24.5 ± 0.4 and 24.6 ± 0.4 hours for *CCA1* and *LHY*, respectively), and also reduced amplitude. A greater reduction in amplitude was observed for transcript levels of both genes in the *gi-2* background (Fig. 3A). This resulted in period estimates (25.7 ± 2.6 and 25.3 ± 2.2 hours for *CCA1* and *LHY*, respectively) that are less precise but consistent with the effects of *gi-2* on *cab2::luc* expression (Table 1 and Fig. 1C).

In sum, the *gi-1* mutation shortened period lengths of leaf movement, *cab2::luc* luminescence, and RNA transcript abundance rhythms. In contrast, *gi-2* caused a shortening of the leaf movement period but caused a gradual lengthening of the luminescence and RNA transcript abundance rhythms. Independent circadian oscillators might separately control different outputs, and GI may affect input pathways feeding into these clocks. Alternatively, the input pathways to a common clock may differ between tissues (for example, leaf blade and petiole), and GI may contribute to these pathways differently in each location.

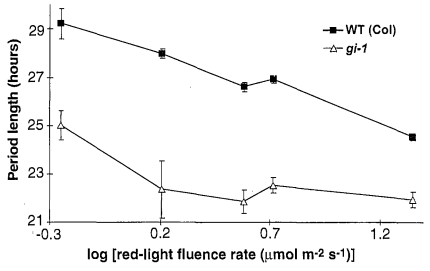

Fig. 4. Effect of red-light fluence rate on free-running period length of *cab2::luc* expression in the wild type and the *gi-1* mutant. Seedlings were entrained as described (*25*), then transferred for >110 hours to continuous red light (600 to 700 nm) at the fluence rates indicated. Period estimates were obtained as previously described (*6, 27*). Error bars indicate ±SEM (n = 8 through 20). Representative data are shown from two independent experiments with similar results.

Of the three components of a circadian system [an input pathway (or pathways), central oscillator, and output pathways (*1, 3*)], GI is unlikely to be a central oscillator component because the putative null mutation (*gi-2*) does not abolish rhythmicity but alters period and reduces amplitude. In wild-type *Arabidopsis*, the free-running period of a circadian clock lengthens with decreasing light intensity in LL (*25*). The rate of period length increase with decreasing light is less in *gi-1* than in the wild type (Fig. 4). This results in an increased relative difference in period lengths between the wild type and mutant at fluence rates between 2 to 5 μmol m^{-2} s^{-1}, consistent with the notion that *gi-1* increases the sensitivity of the circadian system to the controlling effects of light on period length. Only at the lowest intensity tested (0.6 μmol m^{-2} s^{-1}) was there a lengthening of period in *gi-1*, demonstrating that the mutation has shifted the threshold at which light becomes limiting (*16, 25*). This change in the fluence-dependent period lengthening in *gi-1* suggests that GI functions, at least in part, in controlling light signaling to the clock. When we examined the circadian expression pattern of the *GI* gene in continuous darkness (DD) after entrainment in LD (Fig. 3B), the effect of the *gi-2* mutation on the amplitude and sustainability was less severe than that under LL (Fig. 3A). The period-shortening effect of *gi-1* on cycling of the *GI* transcript was also less severe in DD than in LL (Fig. 3B) (*26*). This light-dependent conditional effect of the *gi* mutations further supports the notion that GI functions in a light input pathway.

However, the cyclic expression of the *GI* transcript shows that it is also under circadian control. In the absence of GI in the *gi-2* mutant, the cyclic expression of the *GI* gene as well as known clock-associated genes and simple output genes (for example, *CAB*) shows a reduced amplitude and a gradual increase of period length. Together, these results suggest a model in which GI defines an outer feedback loop that is required to maintain circadian amplitude and proper period length. In this view, yet unidentified circadian clock components would form the core of an oscillator but would be unable to sustain a sufficient amplitude or a proper period length under continuous light to act as a robust timer: An outer feedback loop involving GI could be a mechanism to sustain the necessary amplitude and period length.

References and Notes

1. J. C. Dunlap, *Cell* **96**, 271 (1999); L. D. Wilsbacher and J. S. Takahashi, *Curr. Opin. Genet. Dev.* **8**, 595 (1998); M. Ishiura *et al.*, *Science* **281**, 1519 (1998).
2. J. A. Kreps and S. A. Kay, *Plant Cell* **9**, 1235 (1997); I. A. Carré, *Semin. Cell Dev. Biol.* **7**, 775 (1996); P. Lumsden and A. J. Millar, Eds., *Biological Rhythms and Photoperiodism in Plants* (BIOS, Oxford, 1998).
3. M. W. Young, *Annu. Rev. Biochem.* **67**, 135 (1998); S. K. Crosthwaite, J. C. Dunlap, J. J. Loros, *Science* **276**, 763 (1997); T. Roenneberg and R. G. Foster, *Photochem. Photobiol.* **66**, 549 (1997).
4. G. C. Whitelam and A. J. Millar, in ARABIDOPSIS *Annual Plant Reviews*, M. Anderson and J. A. Roberts, Eds. (CRC Press, Boca Raton, FL, 1998), vol. 1, pp. 331–359.
5. C. H. Johnson *et al.*, *Science* **269**, 1863 (1995).
6. A. J. Millar, S. R. Short, K. Hiratsuka, N.-H. Chua, S. A. Kay, *Plant Mol. Biol. Rep.* **10**, 324 (1992); A. J. Millar, M. Straume, J. Chory, N.-H. Chua, S. A. Kay, *Science* **267**, 1163 (1995).
7. K. A. Hicks *et al.*, *Science* **274**, 790 (1996).
8. Z.-Y. Wang and E. M. Tobin, *Cell* **93**, 1207 (1998); R. M. Green and E. M. Tobin, *Proc. Natl. Acad. Sci. U.S.A.* **96**, 4176 (1999).
9. R. Schaffer *et al.*, *Cell* **93**, 1219 (1998).
10. B. Thomas and D. Vince-Prue, *Photoperiodism in Plants* (Academic Press, San Diego, CA, ed. 2, 1997); R. M. Amasino, *Curr. Opin. Genet. Dev.* **6**, 480 (1996); C. Fankhauser and J. Chory, *Annu. Rev. Cell Dev. Biol.* **13**, 203 (1997).
11. M. Koornneef, C. J. Hanhart, J. H. van der Veen, *Mol. Gen. Genet.* **229**, 57 (1991).
12. M. T. Zagotta *et al.*, *Plant J.* **10**, 691 (1996).
13. G. P. Redei, G. Acedo, G. Gavazzi, *Stadler Genet. Symp.* **6**,135 (1974).
14. T. Araki and Y. Komeda, *Plant J.* **3**, 231 (1993).
15. Period estimates under constant conditions were based on an analysis of the time series between hour 12 and the end of the time course.
16. In *gi-2*, *cab2::luc* expression damped too rapidly at lower fluence rates and longer time courses to obtain reliable period estimates.
17. M. Koornneef *et al.*, *J. Hered.* **74**, 265 (1983).
18. The *th1* mutation has a defect in thiamin monophosphate phosphatase. The *TH1* gene was cloned by functional complementation of an *Escherichia coli* mutation [Y. S. Kim *et al.*, *Plant Mol. Biol.* **37**, 955 (1998)]. The cDNA clone that we initially isolated was from *Brassica napus*. Sequencing of the *Brassica* cDNA clone and a database search revealed an *Arabidopsis* homolog that resides in the *Arabidopsis TH1* locus. The *Brassica* clone, pBTMP1, was used to screen a BAC library of *A. thaliana* [S. Choi, R. A. Creelman, J. E, Mullet, R. A. Wing, *Plant Mol. Biol. Rep.* **13**, 124 (1995)].
19. See Web figure 1 (available at www.sciencemag.org/feature/data/1041930.shl).
20. The two fragments were isolated from the T22J18 clone.
21. M. Seki, P. Carninci, Y. Hayashizaki, K. Shinozaki, *Plant J.* **15**, 707 (1998).
22. The ORF of the cDNA sequence showed a minor difference from the ORF predicted from the genomic sequence.
23. The mean variance-weighted periods and associated variance-weighted SD (*6*) for *GI*, *CCA1*, and *LHY* cycling transcript levels were obtained from three independent trials with fast Fourier transform–nonlinear least squares (FFT-NLLS) curve-fitting software (*27*). The low amplitude of the *gi-2* data did not allow precise period estimates, and we cannot exclude the possibility that these rhythms are rapidly damping to arrhythmicity. However, the results are consistent with the lengthening of period seen in the more highly resolved luminescence rhythms (Table 1).
24. R. Allada, N. E. White, W. V. So, J. C. Hall, M. Rosbash, *Cell* **93**, 791 (1998); T. K. Darlington *et al.*, *Science* **280**, 1599 (1998); B. D. Aronson, K. A. Johnson, J. J. Loros, J. C. Dunlap, *ibid.* **263**, 1578 (1994); N. Gekakis *et al.*, *ibid.* **280**, 1564 (1998).
25. D. E. Somers, P. F. Devlin, S. A. Kay, *Science* **282**, 1488 (1998); D. E. Somers, A. A. Webb, M. Pearson, S. A. Kay, *Development* **125**, 485 (1998).
26. Variance-weighted period estimates and the asso-

ciated variance-weighted SD (6) of the cycling of *GI* transcript levels in wild-type (23.9 ± 1.9 hours), *gi-1* (22.9 ± 1.5 hours), and *gi-2* (25.5 ± 4.6 hours) backgrounds were obtained from two independent trials with FFT-NLLS curve-fitting software (27). In extended DD, *LHY* transcript levels were too low or the time series were too short to obtain reliable period estimates. *CCA1* expression is reported to damp rapidly in DD (8) and was not considered here.

27. J. D. Plautz *et al.*, *J. Biol. Rhythms* **12**, 204 (1997).
28. An F_2 population (n = 71) of seedlings segregating for *gi-1* [*gi-1* (Col) × 2CAC] (6) and an F_2 population (n = 36) of seedlings segregating for *gi-2* {[*gi-2* (Col) × 2CAC F_3] × Col} were scored for the correlation between the luminescence-based circadian phenotype and the presence of either a 5-bp deletion in *gi-1* or for a 7-bp deletion in *gi-2*. Each genotype was identified by PCR with primer pairs that uncovered a 5-bp deletion in *gi-1* (primer pairs, 5′-GGAGTTGCAGCCTTGGATCG-3′ and 5′-AGATCTGATGCACTTGCGAG-3′) and a 7-bp deletion in *gi-2* (primer pairs, 5′-CAGAATGACTATTCGGAGCA-3′ and 5′-GGAGAACCACTAGTTGTAGC-3′).
29. J. M. Kwak *et al.*, *Planta* **201**, 245 (1997).
30. This work was supported by grants from the Korean Ministry of Agriculture to H.G.N., from NSF to S.A.K. (grant MCB-9724120), and from NIH to S.A.K. (grant GM56006). D.E.S. was supported, in part, as an NSF Postdoctoral Fellow in Plant Biology (grant BIR-9403981).

19 May 1999; accepted 4 August 1999

Real-Time Tracking of Memory Formation in the Human Rhinal Cortex and Hippocampus

Guillén Fernández,[1]* Arndt Effern,[1,2] Thomas Grunwald,[1] Nico Pezer,[1] Klaus Lehnertz,[1] Matthias Dümpelmann,[1] Dirk Van Roost,[3] Christian E. Elger[1]

A fundamental question about human memory is which brain structures are involved, and when, in transforming experiences into memories. This experiment sought to identify neural correlates of memory formation with the use of intracerebral electrodes implanted in the brains of patients with temporal lobe epilepsy. Event-related potentials (ERPs) were recorded directly from the medial temporal lobe (MTL) as the patients studied single words. ERPs elicited by words subsequently recalled in a memory test were contrasted with ERPs elicited by unrecalled words. Memory formation was associated with distinct but interrelated ERP differences within the rhinal cortex and the hippocampus, which arose after about 300 and 500 milliseconds, respectively. These findings suggest that declarative memory formation is dissociable into subprocesses and sequentially organized within the MTL.

How do brain processes during an experience that will be remembered differ from those during an experience that will be forgotten? Answering this question might elucidate memory formation or memory encoding, a process transforming sensory representations of an experience into the code of the declarative memory system. This system mediates conscious recollection of past events and facts (*1, 2*). It depends on the structural integrity of the MTL (*3*), and neuroimaging studies suggest that the MTL plays a crucial role during memory formation (*4, 5*). Efferences from association areas enter the MTL primarily via the perirhinal and parahippocampal cortices, providing the major input to the entorhinal cortex, which in turn provides the main input to the hippocampus (*6*). However, imaging (*7*), patient (*8*), and animal studies (*1, 9*) have produced inconsistent results regarding specific functions of and interactions between MTL substructures. This inconsistency has given rise to different ideas about the organizational structure of the MTL memory system, contrasting a rather unitary model with modular models featuring either serial or parallel processing modes (*1, 9*).

The question of when the process of declarative memory formation is initiated also remains unresolved. Neural processing at the time of stimulus encoding is critical for later retrievability (*10*), and functional magnetic resonance imaging (MRI) has offered evidence for time-locked posterior parahippocampal activity related to subsequent memory performance (*4*). Yet the exact time course of this activity cannot be assessed by this technique because functional MRI is based on indirect, hemodynamic measures. By contrast, ERPs enable direct, real-time monitoring of brain activity. Scalp ERPs recorded at the time of stimulus encoding and associated with subsequently recalled words begin to separate from those associated with subsequently forgotten words about 200 ms after stimulus onset (*11, 12*). This subsequent memory effect or difference due to memory (dm-effect) (*11*) has been differentiated from processes of implicit memory, semantic processing, and detection of distinctiveness (*12*). Hence, this effect may be related specifically to declarative memory formation. However, it remains unclear where this effect is generated because the generators of scalp ERPs are notoriously difficult to localize (*13*). ERPs recorded invasively from depth electrodes placed directly into the MTL eliminate or mitigate the limitations of scalp-recorded ERPs and functional MRI by combining their advantages: direct measure of neural activity, real-time temporal resolution, and fine-grained spatial resolution within the MTL (*14, 15*).

In certain patients with medically refractory temporal lobe epilepsy, it is necessary to insert bilateral depth electrodes to define the zone of seizure origin for resective surgery (Fig. 1). If seizures are proved to originate unilaterally, contralateral electrodes enable recordings of MTL activity unrelated to epilepsy (*16*). We set out to use ERP recordings from such nonepileptic MTLs to define the time course of the initial steps of human declarative memory formation. Because electrodes enabled separate recordings within the hippocampus and the anterior parahippocampal gyrus (Figs. 1 and 2), we also examined whether memory formation is dissociable into subprocesses performed by these structures.

We recorded ERPs invasively (*17*) from 12 patients (*18*) with unilateral temporal lobe epilepsy (*19*). Each patient participated in 20 study-test blocks of a direct single-trial word

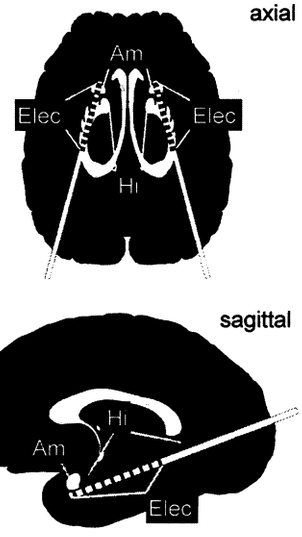

Fig. 1. Schematic drawings of multicontact depth electrodes reaching the anterior parahippocampal gyrus and the hippocampus on both sides (Am, amygdala; Elec, electrode; Hi, hippocampus).

[1]Department of Epileptology, [2]Department of Radiation and Nuclear Physics, [3]Department of Neurosurgery, University of Bonn, 53105 Bonn, Germany.

*To whom correspondence should be addressed. E-mail: gf@mailer.meb.uni-bonn.de